Advances in Agriculture

SPECIAL ISSUE Advances in Drying Technologies for Perishable Commodities: Innovations, Efficiency, and Quality Improvement

RESEARCH ARTICLE OPEN ACCESS

Ultrasonication-Assisted Hot-Air Drying of Tomato Slices: Impact on Drying Kinetics and Thermodynamic Properties, Energy Consumption, and Quality Attributes

Eyitayo Kehinde Oladipo[1,2] | Zinash A. Belay[1,3] | Oluwafemi James Caleb[1,2]

[1]Department of Food Science, Faculty of AgriSciences, Stellenbosch University, Private Bag X1, Stellenbosch 7599, South Africa | [2]AgriFood BioSystems and Technovation Research Group, Africa Institute for Postharvest Technology, Faculty of AgriSciences, Stellenbosch University, Private Bag X1, Stellenbosch 7599, South Africa | [3]Agri-Food Systems and Omics Laboratory, Post-Harvest and Agro-Processing Technologies (PHATs), Agricultural Research Council (ARC) Infruitec-Nietvoorbij, Private Bag X5026, Stellenbosch 7599, South Africa

Correspondence: Oluwafemi James Caleb (caleboj@sun.ac.za)

Received: 17 December 2025 | **Revised:** 28 March 2026 | **Accepted:** 20 June 2026

Guest Editor: Deepika Kohli

Keywords: activation energy | moisture diffusivity | phenolic content | thin-layer drying | tomato

ABSTRACT

Tomatoes are highly perishable due to their high-moisture content, requiring effective preservation to extend shelf life. This study investigated the effects of ultrasound pretreatment combined with hot-air drying on the drying kinetics, thermodynamic properties, energy consumption, and quality attributes of tomato slices. Samples were pretreated with ultrasound for 20 min (U-20) and 40 min (U-40), then dried at 40, 50, and 60°C, and compared with untreated controls. Among seven thin-layer models evaluated, the Midilli–Kucuk et al.'s model provided the best fit in most conditions ($R^2 = 0.9942$–0.9993). Effective moisture diffusivity ranged from 3.02×10^{-10} to 7.94×10^{-10} m^2/s, increasing with temperature, while activation energy decreased from 39.86 kJ/mol in the control to 33.28 and 31.28 kJ/mol in U-20 and U-40, respectively, confirming that ultrasonication lowered the diffusion energy barrier. Thermodynamic analysis revealed that ultrasound lowered the enthalpic barrier and promoted molecular ordering, while positive Gibbs free-energy values confirmed that drying remained nonspontaneous across all conditions. Total specific energy consumption decreased with increasing temperature, with moderate ultrasound exposure (U-20) achieving the greatest savings compared with the control, particularly under mild drying conditions. Quality analyses showed that U-20 minimized shrinkage, improved rehydration, and best-preserved color ($\Delta E = 6.75$ at 60°C), whereas prolonged sonication (U-40) caused over-disruption. Overall, 20 min ultrasound pretreatment optimally enhanced drying efficiency, reduced energy demand, and maintained the structural and visual quality of dried tomato slices.

1 | Introduction

Nutritionally, tomatoes are highly regarded for their rich composition of essential micronutrients and health-promoting compounds. They supply appreciable amounts of vitamin C, potassium, and folate, nutrients that play vital roles in immune defense, cardiovascular well-being, and cellular development and repair. In addition, tomatoes are rich in lycopene, a potent antioxidant, while their high water content enhances hydration [1].

However, tomatoes are highly perishable because of their high-moisture content (90%–95%), which makes them susceptible to decay, rot, and fungal growth, causing substantial economic losses for farmers, processors, and consumers during postharvest

This is an open access article under the terms of the Creative Commons Attribution License, which permits use, distribution and reproduction in any medium, provided the original work is properly cited.

Copyright © 2026 Eyitayo Kehinde Oladipo et al. *Advances in Agriculture* published by John Wiley & Sons Ltd.

handling and storage. Globally, these losses account for about 23% of harvested tomatoes in developed countries and up to 50% in developing regions [1, 2]. This loss limits their availability and affordability, particularly in developing regions where tomatoes are a key dietary staple. Thus, reducing postharvest losses is critical.

Drying is one of the most common preservation methods for agricultural products as it lowers moisture content, suppresses enzymatic and microbial activity, extends shelf life, and reduces packaging and transportation costs [3, 4]. Among the various approaches, such as conventional sun drying, solar drying, and fluidized-bed drying, hot-air oven drying is often preferred because it offers controlled air temperature and velocity, ensuring greater hygiene and uniformity [5]. However, hot-air drying is energy-intensive, and the prolonged thermal exposure often compromises the structural and nutritional quality of the dried product, necessitating the use of pretreatments to improve the process efficiency.

During drying, the delicate structure of tomatoes often causes shrinkage, color loss, and nutrient degradation [6, 7]. To minimize these effects, pretreatments, such as blanching [8], osmotic dehydration [9], or chemical dipping [10], can improve moisture removal and drying efficiency. However, these methods may reduce key nutrients like vitamin C and phenolics [10, 11]. To overcome such limitations, innovative approaches like ultrasound pretreatment have gained attention.

Ultrasonication involves immersing fruits or vegetables in water or hypertonic solutions while applying sound waves, which generate microscopic cavitation bubbles that disrupt cell walls [12, 13]. This disruption enhances moisture diffusion and reduces the drying time. The pretreatment can be carried out at ambient temperature, which is advantageous for preserving heat-sensitive compounds. Previous studies reported that ultrasound pretreatment of fruits enhances the drying efficiency [14–16], reduces energy consumption depending on the duration applied [17, 18], and improves antioxidant activity in the dried products [16, 19]. For instance, Wang et al. [19] observed improved antioxidant activity in hot-air drying of kiwifruit after ultrasound pretreatment. Jahanbakhshi et al. [17] reported a reduction in the energy demand for nectarine drying from 212.97 to 59.70 kWh/kg. Cao et al. [15] found that ultrasound pretreatment shortened litchi drying time by nearly 50%.

Although several studies have examined thin-layer drying models for tomatoes [20–23], a comprehensive investigation that simultaneously links ultrasound pretreatment with thermodynamic drying behavior, specific energy consumption, and multiparameter product quality assessment during hot-air drying of tomato slices remains lacking. In particular, the thermodynamic implications of ultrasound-induced structural changes, including enthalpy, entropy, and Gibbs free energy of activation, have not been examined for tomato drying, and the energy trade-off between ultrasound pretreatment intensity and oven drying energy savings has not been systematically quantified. Addressing these gaps is essential for establishing whether ultrasound pretreatment represents a genuinely energy-efficient and quality-preserving processing strategy for tomatoes. Therefore, this study investigated the combined effects of ultrasonication duration (20 and 40 min) and drying temperature (40, 50, and 60°C) on the drying kinetics, thermodynamic properties, specific energy consumption, and quality attributes of tomato slices to identify the optimal pretreatment condition for efficient and high-quality hot-air drying.

2 | Materials and Methods

2.1 | Sample Collection

Fresh "SV6112" round tomatoes (*Solanum lycopersicum*) used in this study were obtained from a single local supplier at Rennie Farms, Kliprug Minor Road, Paarl, Western Cape, South Africa. Tomatoes with uniform sizes and firmness were selected at maturity stage 5 (with ~5% of the pulp unripe, total soluble solids (TSS, 3.4 ± 0.02 °Brix), titratable acidity (TA, 0.4 ± 0.01 g/100 mL), pH 4.6 ± 0.09, and an initial moisture content of $94.58 \pm 0.26\%$). The fruits were transported to AgriFood BioSystems and Laboratory, Stellenbosch, South Africa. All reagents and chemicals employed in the study were of analytical grade.

2.2 | Processing and Pretreatment of Tomato Slices

The tomatoes were washed with cold tap water to remove surface dirt and potential contaminants, drained, and then sliced using a Mandoline Food Slicer (Model: MAS0001, Matt Catering Equipment, KZN, South Africa) to an average thickness of 6 mm to ensure uniform drying and efficient moisture diffusion. The seeds were not removed during drying because they contain bioactive compounds that contribute to their overall nutritional and antioxidant properties. The fresh tomato samples were analyzed for moisture content, color, pH, TA, TSS, and total phenolic content (TPC).

Ultrasound pretreatment of tomato slices was performed in a 30 L capacity ultrasonic bath (Model: DC400/DC400H, Delta Ultrasonic Co., Ltd., New Taipei City, Taiwan) operating at 40 kHz and 400 W. Samples were immersed in water at a tomato-to-water ratio of 1:4, with the bath temperature maintained at 25 ± 2°C to prevent the degradation of heat-sensitive compounds. The water was refreshed between treatments to avoid localized heating. Pretreatment durations of 20 min (U-20) and 40 min (U-40) were applied, representing short and extended exposure times [17]. After sonication, excess surface water was drained before hot-air oven drying.

2.3 | Hot-Air Oven Drying, Moisture Ratio, and Drying Rate

The sliced tomato was divided into two groups: untreated (control) and ultrasound-pretreated samples sonicated for 20 min (U-20) and 40 min (U-40), respectively. For each run, 100 g of slices was evenly spread in a single thin layer on drying trays (tray area: 0.089 m^2; 325 mm × 275 mm) without overlapping to ensure uniform air circulation and moisture transfer. Three independent replicates were performed per treatment. Drying was carried out in a forced-draft hot-air oven (Model: 363, ThermoScientific, Waltham, MA, USA) at set temperatures of 40, 50, and 60°C with an air velocity of 1.5 m/s. The oven was preheated to the target temperature for 30 min before sample loading to ensure thermal stability. Moisture loss was recorded hourly using a precision balance (MS3002S New Classic MF, Mettler Toledo, Columbus, OH, USA; readability ± 0.01 g), and drying continued until the mass change was <0.1 g over two successive readings, indicating that equilibrium moisture content had been reached.

To examine the effects of ultrasound pretreatment and drying temperature on tomato-slice drying behavior, nine treatment combinations were used as follows: 40°C – control, 40°C (U-20), 40°C (U-40); 50°C – control, 50°C (U-20), 50°C (U-40); and 60°C – control, 60°C (U-20), 60°C (U-40). The mass-time data obtained from each set of experiments were converted to moisture content-drying time data. The moisture content of tomato slices at time t, X_t (g water/g dry matter), is calculated as given in Equation (1) [24].

$$X_t = \frac{m_t - m_d}{m_d}, \tag{1}$$

where m_t and m_d represent the mass (g) of the tomato sample at any time t and mass (g) of the dried sample, respectively.

The drying rate, D_R (g water/g dry matter. min) of tomato slices was calculated as given in Equation (2) [24].

$$D_R = \frac{X_{t+dt} - X_t}{dt}, \tag{2}$$

where X_{t+dt} is the moisture content at time $t+dt$ (g water/g dry matter), and dt is the time increment (min).

The moisture content can be expressed as a dimensionless moisture ratio (M_R), as shown in Equation (3) [24].

$$M_R = \frac{X_t - X_e}{X_i - X_e}, \tag{3}$$

where X_i and X_e represent the initial and equilibrium moisture contents, respectively.

Since the value of X_e is relatively small for a long drying time when compared to X_t and X_i, it is considered negligible [25]. Thus, the expression can be further simplified, as shown in Equation (4).

$$M_R = \frac{X_t}{X_i}. \tag{4}$$

2.4 | Thin-Layer Mathematical Modeling of Drying Kinetics

Experimental data of M_R versus t for each drying condition were fitted to seven thin-layer drying models, namely, Lewis [26], Page [27], Henderson and Pabis [28], Logarithmic [29], Midilli–Kucuk et al. [30], Verma et al. [31], and Modified Verma et al. reported by Wang et al. [32] (Table 1), using nonlinear regression in OriginPro 2024 (OriginLab Corp., Northampton, MA). Model performance was evaluated using the coefficient of determination (R^2), the reduced chi-square (χ^2), and the root mean square error (RMSE). The best-fit model between the predicted and experimental data was assessed based on higher R^2, lower χ^2, and RMSE values. The parameters were calculated according to standard expressions, as shown in Equations (5)–(7), respectively.

$$R^2 = 1 - \frac{\sum_{i=1}^{N}\left(M_{R_{\text{exp,i}}} - M_{R_{\text{pre,i}}}\right)^2}{\sum_{i=1}^{N}\left(M_{R_{\text{exp,i}}} - M_{R_{\text{exp(avg),}i}}\right)^2}, \tag{5}$$

TABLE 1 | Thin-layer drying models fitted to drying data products.

Number	Model name	Model equation[a]	References
1	Lewis	$M_R = \exp(-kt)$	[26]
2	Page	$M_R = \exp(-kt^n)$	[27]
3	Henderson and Pabis	$M_R = a\exp(-kt)$	[28]
4	Logarithmic	$M_R = a\exp(-kt) + c$	[29]
5	Midilli et al.	$M_R = a\exp(-kt^n) + bt$	[30]
6	Verma et al.	$M_R = a\exp(-kt) + (1-a)\exp(-gt)$	[31]
7	Modified Verma et al.	$M_R = a\exp(-k_0t^n) + (1-a)\exp(-k_1t^n)$	[32]

[a]Model constants: a, dimensionless fitting parameter; k, k_0, k_1, g, drying rate constants (h^{-1}); n, dimensionless exponent; b, linear drying coefficient (h^{-1}); c, additive equilibrium constant (dimensionless).

$$\chi^2 = \frac{\sum_{i=1}^{N}\left(M_{R_{\text{exp,i}}} - M_{R_{\text{pre,i}}}\right)^2}{N-n}, \tag{6}$$

$$\text{RMSE} = \sqrt{\frac{\sum_{i=1}^{N}\left(M_{R_{\text{pre,i}}} - M_{R_{\text{exp,i}}}\right)^2}{N}}, \tag{7}$$

where N is the number of observations, n is the number of constants in the drying equation, and $M_{R(exp,i)}$ and $M_{R(pre,\ i)}$ represent the ith experimental and predicted M_R, respectively.

2.5 | Drying Kinetics and Thermodynamic Properties

2.5.1 | Effective Moisture Diffusivity

The effective moisture diffusivity, D_{eff} (m^2/s), was determined from the drying data using Fick's second law of diffusion, which describes internal moisture migration during the falling-rate drying period when internal mass transfer is the controlling mechanism [33]. Assuming uniform initial moisture distribution and constant diffusion coefficients, the analytical solution for a slab geometry [34] was simplified to the first term of the general diffusion expression, as in Equation (8) [35].

$$M_R = \frac{8}{\pi^2}\exp\left(-\frac{\pi^2 D_{\text{eff}} t}{4L^2}\right), \tag{8}$$

where L is half of the thickness of the sample (m) and t is the time of drying (min). D_{eff} was calculated from the slope of the linear plot of ln (M_R) vs. time (t) as expressed in Equation (9) [36].

$$\ln(M_R) = \ln\left(\frac{8}{\pi^2}\right) - \left(\frac{\pi^2 D_{\text{eff}} t}{4L^2}\right). \tag{9}$$

2.5.2 | Determination of Activation Energy

The activation energy, E_a (kJ/mol), is the minimum amount of energy required to initiate the drying process. The temperature dependence of D_{eff} was expressed by the Arrhenius equation (Equation 10) [24]

$$D_{\text{eff}} = D_0 \exp\left(-\frac{E_a}{\text{RT}}\right), \tag{10}$$

where D_0 (m^2/s) is the pre-exponential factor of the Arrhenius equation, R is the universal gas constant (8.314 J/mol.K), and T is the absolute drying temperature (K).

Taking the natural logarithm yields a linear relationship between ln (D_{eff}) and $1/T$, from which E_a was obtained from the slope of the fitted line (Equation 11).

$$\ln(D_{\text{eff}}) = \ln(D_0) - \frac{E_a}{R}\frac{1}{T}. \tag{11}$$

2.5.3 | Enthalpy, Entropy, and Gibbs Free Energy of Activation

Thermodynamic analysis provides insights into the energy barrier and molecular ordering that govern the drying process and helps assess the balance between moisture removal efficiency and energy demand. Thermodynamic parameters associated with moisture diffusion: enthalpy change $\Delta H^{\dagger}$ (kJ/mol), entropy change $\Delta S^{\dagger}$ (J/mol.K), and Gibbs free-energy change $\Delta G^{\dagger}$ (kJ/mol), were estimated using the Eyring transition-state theory derived from the Arrhenius equation, as shown in Equations (12)–(14) [37, 38].

$$\Delta H^{\dagger} = E_a - RT, \tag{12}$$

$$\Delta S^{\dagger} = R\left(\ln D_0 - \ln\frac{k_B}{h} - \ln T\right), \tag{13}$$

$$\Delta G^{\dagger} = \Delta H^{\dagger} - T\Delta S^{\dagger}, \tag{14}$$

where k_B is the Boltzmann's constant (1.38×10^{-23} J/K) and h is Planck's constant (6.63×10^{-34} Js).

2.5.4 | Total Specific Energy Consumption

The ultrasound power, P_U (kW), was determined from the electrical input parameters using Equation (15) [17].

$$P_{\text{U}} = UI\cos\theta, \tag{15}$$

where U is the voltage (V), I is the current (A) applied to the ultrasound generator, θ is the phase angle, and cos θ is the power factor considered to be 0.8.

The corresponding energy used, E_{U} (kWh), by the ultrasound instrument over time (t) and its specific energy consumption, E_{SPU} (kWh/kg), were calculated using Equations (16) and (17) [17, 24].

$$E_{\text{U}} = P_{\text{U}} \times t, \tag{16}$$

$$E_{\text{SPU}} = \frac{E_{\text{U}}}{m_i - m_d}, \tag{17}$$

where m_i and m_d are the initial mass (kg) and oven-dry mass of tomato slices (kg), respectively.

The energy consumed by the hot-air oven, E_O (kWh), was computed based on the thermal energy required to heat air across the drying chamber, as shown in Equation (18), while the specific energy consumption, E_{SPO} (kWh/kg), representing the energy required to dry 1 kg of ultrasound-pretreated sample, was calculated using Equation (19) [17, 24].

$$E_{\text{O}} = A\upsilon\rho_a c_a \Delta T D_t, \tag{18}$$

where A represents the tray area (m^2), υ denotes the air velocity (m/s), ρ_a is the air density (kg/m^3), c_a is the specific heat capacity of air (kJ/kg °C) at each temperature, ΔT is the temperature difference (°C), and D_t is the total drying time (h) for the sample.

$$E_{\text{SPO}} = \frac{E_{\text{O}}}{m_i - m_d}. \tag{19}$$

The total specific energy consumption (E_{T}), representing the overall energy demand for ultrasonication and hot-air drying, is obtained from Equation (20).

$$E_{\text{T}} = E_{\text{SPU}} + E_{\text{SPO}}. \tag{20}$$

2.6 | Quality Attributes

2.6.1 | Color Determination

Color change during drying reflects chemical and pigment transformations that influence product quality and consumer acceptability [39]. Color attributes of the dried tomato slices were measured in the *CIE* $L^*a^*b^*$ color space using a digital colorimeter (Minolta CR-400, Tokyo, Japan). The overall color difference (ΔE^*_{ab}) between fresh and dried samples was calculated from Equation (21) [40].

$$\Delta E^*_{ab} = \sqrt{(\Delta L^*)^2 + (\Delta a^*)^2 + (\Delta b^*)^2}, \tag{21}$$

where ΔL^*, Δa^*, and Δb^* represent changes in brightness, red–green intensity, and yellow–blue intensity of the tomato slices before and after drying, respectively.

2.6.2 | TPC

The TPC of tomato samples was determined using the Folin–Ciocalteu method with minor modifications [41]. Briefly, 500 µL of tomato extract (50 mg/mL) was mixed with 500 µL of the Folin–Ciocalteu reagent and 450 µL of 50% methanol. After standing for 20 min, 2.0 mL of 7.5% (w/v) sodium carbonate solution was added, and the mixture was incubated in the dark for 1 h. Absorbance was measured at 765 nm using a UV–Vis spectrophotometer (SP–UV 300 Series, PerkinElmer, Semenyih, Malaysia). Gallic acid was used as the standard, and TPC was expressed as mg gallic acid equivalent (GAE)/g dry weight (DW), as expressed in Equation (22).

$$\text{TPC (mg GAE/gDW)} = \frac{c \times V}{m}, \tag{22}$$

where c is the concentration of phenolics (mg GAE/mL), V is the total volume of the extract (mL), and m is the dry mass of the sample extracted (g).

2.6.3 | Shrinkage Determination

Structural shrinkage resulting from drying was determined from the change in the sample volume before and after dehydration. Volumes were measured by toluene displacement, which avoids water uptake and minimizes surface-tension errors. After drying, the samples were equilibrated to room temperature before measurement. The shrinkage (%) was calculated using Equation (23) [18].

$$\text{Shrinkage}\,(\%) = \frac{V_0 - V_d}{V_0} \times 100, \tag{23}$$

where V_0 is the initial volume (mL) of the fresh sample, and V_d is the volume (mL) after drying.

2.6.4 | Rehydration Ratio (RR)

Rehydration ability, which reflects the structural integrity and water-absorption capacity of dried tomato slices, was evaluated by immersing a known mass of dried samples in distilled water at a 1:50 (w/v) ratio. Rehydration was carried out at 25 ± 1°C for 60 min, a duration established from preliminary trials in which mass measurements taken at 5 min intervals confirmed that water absorption reached a plateau, indicating the attainment of equilibrium. After rehydration, excess surface water was removed by blotting, and the samples were weighed. The RR was calculated using Equation (24) [39].

$$\text{RR} = \frac{W_r}{W_d}, \tag{24}$$

where W_r and W_d represent the masses (g) of the rehydrated and dried samples, respectively.

2.7 | Statistical Analysis

A two-way analysis of variance (ANOVA) was performed under a completely randomized design to evaluate the effects of drying temperature (Factor A: 40, 50, and 60°C), ultrasound pretreatment duration (Factor B: 0, 20, and 40 min), and their interaction on the total color difference, TPC, shrinkage, and RR of dried tomato slices. All treatment combinations were performed in triplicate. Where significant differences were detected, mean separations were carried out using Tukey's post-hoc test at a significant level of $p < 0.05$. Pearson's correlation analysis was used to assess relationships among variables, where r indicates the correlation strength and direction and p denotes significance. Statistical analyses were conducted using JASP software (Version 0.18.3), and all results are expressed as mean ± standard deviation.

3 | Results and Discussion

3.1 | Effect of Ultrasonic Pretreatment and Temperature on Drying Time

At 40°C, the time to reach equilibrium moisture content was 15 h for both the untreated and U-40 pretreated samples, while U-20 pretreatment shortened the duration to 14 h (a 6.7% reduction) (Figure 1a). A similar trend was observed at 50°C (Figure 1b), where the untreated and U-40 samples dried within 12 h, while the 20 min pretreatment reduced the drying time by 8.3%. The enhanced efficiency of U-20 pretreated samples is attributable to ultrasound-induced cavitation, which generates microscopic pores and disrupts the cellular structure, thereby facilitating internal water diffusion and surface evaporation [42]. However, extended sonication for 40 min likely weakened tissue integrity, leading to structural collapse and impaired capillary flow, offsetting the benefits of ultrasound [12].

At 60°C, the influence of ultrasonication on drying time became negligible as all samples, treated and untreated, reached equilibrium moisture content within 9 h (Figure 1c). At this elevated temperature, the strong vapor pressure gradient between the product and the drying air accelerates water removal to the extent that the incremental effect of ultrasound becomes negligible. These findings suggest that moderate ultrasonication (20 min) is more effective than prolonged exposure (40 min) for reducing drying duration and improving mass transfer, particularly under mild drying conditions, whereas its impact diminishes at higher temperatures.

3.2 | Performance of Thin-Layer Drying Models

Experimental data and the best-fit predicted model for all the drying conditions investigated are summarized in Supporting Information Figure S1. Across all drying conditions, the Midilli–Kucuk et al.'s [30] model generally provided the best description of tomato-slice drying behavior (Table 2). This model achieved excellent fits in seven of the nine treatment combinations, with R^2 values ranging from 0.9942 to 0.9993 and very low RMSE (0.0064–0.0264) and χ^2 (5.54×10^{-5}–1.17×10^{-3}). The superior performance of the Midilli–Kucuk et al.'s [30] model can be attributed to its mathematical structure, which combines a Page-type exponential term with a linear correction term (bt) that accommodates the slow residual moisture removal characteristic of the late falling-rate period. Tomato slices are high-moisture, structurally complex biological tissues in which moisture does not migrate through a single uniform pathway, transitioning from relatively rapid early-stage moisture removal to progressively slower internal diffusion as drying proceeds. Consequently, simpler single-term models such as Lewis or Henderson and Pabis cannot adequately represent this transition, whereas the Midilli–Kucuk et al.'s [30] model has the flexibility to describe the full drying trajectory across all temperature and pretreatment conditions investigated. The suitability of this model for tomato-slice drying is well established in the literature [43, 44].

The logarithmic model performed best for the 40°C (U-20) and 50°C (U-20) conditions. The model includes an additive constant that captures an asymptotic approach to equilibrium moisture content, consistent with a gradual slowdown in moisture removal as the product approaches its equilibrium state. This behavior is expected when moderate ultrasound pretreatment creates microchannels in the tissue matrix that facilitate moisture migration without compromising structural integrity [45]. In contrast, prolonged sonication (U-40) may induce structural over-disruption that impairs capillary continuity, reducing the efficiency of moisture transport and shifting the best-fit model back toward the Midilli–Kucuk structure. These model transitions indicate that ultrasound duration modulates internal moisture transport pathways in a duration-dependent manner. The role of cavitation-induced microchannels in facilitating this moisture migration

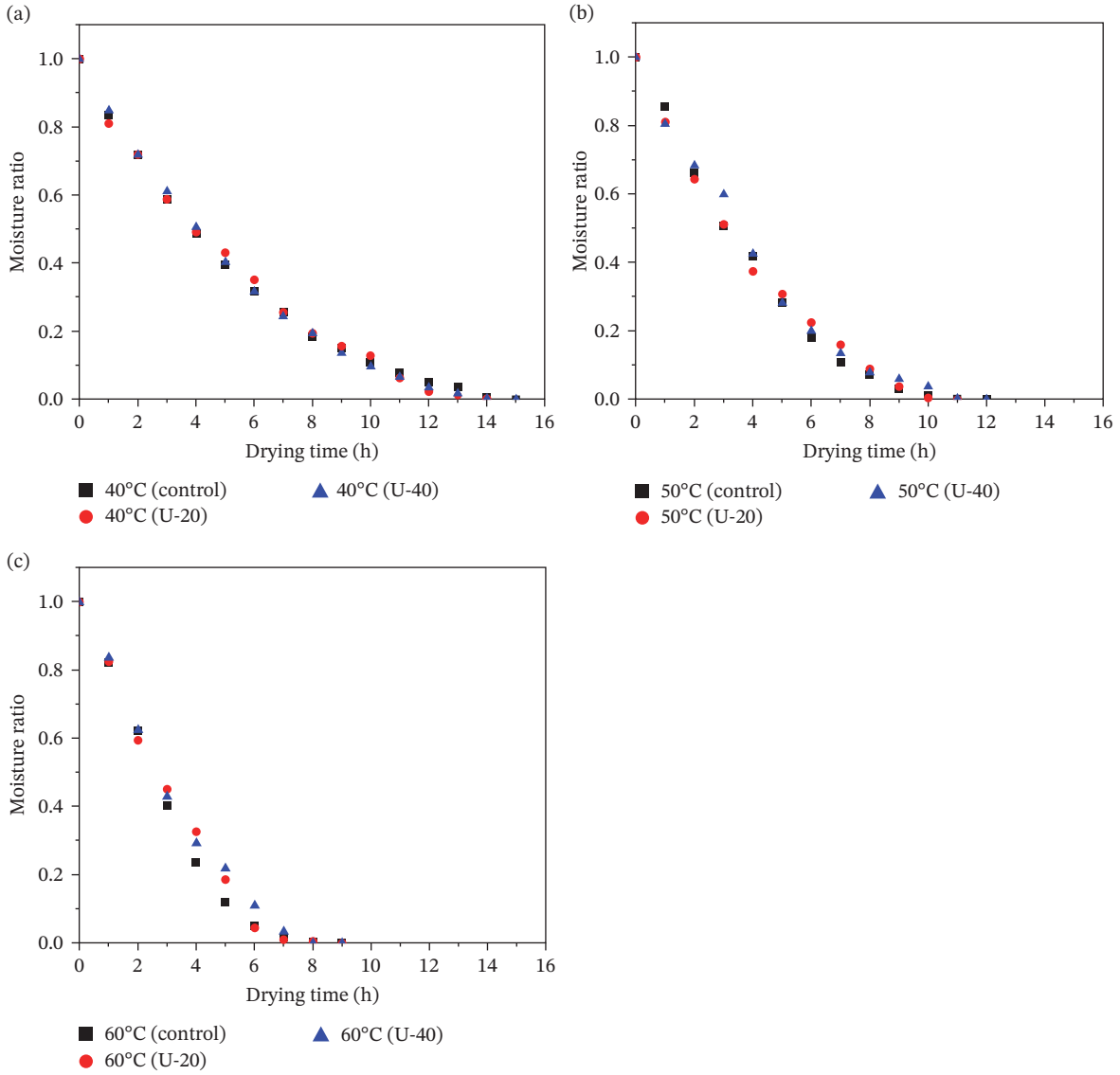


FIGURE 1 | Drying curves showing moisture ratio as a function of drying time for tomato slices subjected to ultrasound pretreatment (U-20 and U-40) and untreated controls at (a) 40, (b) 50, and (c) 60°C.

has been reported in the literature. Jahanbakhshi et al. [17] attributed enhanced moisture transport in ultrasound-pretreated nectarine to cavitation-induced sponge-like structural changes and microchannel formation, while Abbaspour-Gilandeh et al. [39] similarly reported that ultrasound pretreatment facilitated moisture release through cavitation in cantaloupe slices. The results in this study indicate that tomato-slice drying is primarily governed by internal moisture diffusion, with ultrasound-induced structural modification playing a modulating role, while external mass-transfer resistance remains minor throughout.

3.3 | Effect of Ultrasound Pretreatment and Temperature on Effective Moisture Diffusivity

The values of D_{eff} obtained for tomato slices in this study ranged from 3.02×10^{-10} to 7.94×10^{-10} m^2/s, depending on the drying temperature and ultrasound pretreatment (Figure 2). D_{eff} values increased with temperature under all conditions, indicating that higher thermal energy enhances internal moisture transport by intensifying the vapor pressure gradient, increasing water-molecule mobility, and reducing viscosity [41, 46, 47]. At 40°C, U-20 and U-40 increased D_{eff} by 21.5% and 25.5% relative to the control, respectively. At 50°C, however, both pretreatments slightly reduced D_{eff} relative to the control, possibly because cavitation-induced tissue softening at this intermediate temperature partially disrupted capillary continuity, temporarily impeding moisture flow. This effect became negligible at 60°C, where the dominant thermal driving force overrode structural influences, as reflected in the minimal differences observed (≤5.2%). This pattern suggests that ultrasound-induced structural modifications improve water migration primarily under low-thermal conditions. In contrast, at higher temperatures, the strong thermal driving force dominates moisture transfer, diminishing the relative contribution of ultrasound [48, 49].

From a drying efficiency perspective, higher D_{eff} values are desirable because they correspond to faster internal water migration, shorter drying times, and potentially lower energy demand [49, 50]. In this study, the highest D_{eff} was recorded at 60°C (U-20) (7.94×10^{-10} m^2/s), while the lowest occurred at 40°C (control) (3.02×10^{-10} m^2/s). These results also confirm that D_{eff} increased

TABLE 2 | Best-fit thin-layer model for each drying condition, with statistical parameters.

Condition	Best model	Model constants	R^2	RMSE	χ^2
40°C – control	Midilli et al. [30]	$a = 0.9940$, $k = 0.1517$, $n = 1.0924$, $b = -0.0039$	0.9996	0.0064	0.0000554
40°C (U-20)	Logarithmic	$a = 1.1910$, $k = 0.1322$, $c = -0.2055$	0.9977	0.0148	0.000273
40°C (U-40)	Midilli et al. [30]	$a = 0.9903$, $k = 0.1317$, $n = 1.1677$, $b = -0.0039$	0.9993	0.00816	0.0000888
50°C – control	Midilli et al. [30]	$a = 0.9963$, $k = 0.1515$, $n = 1.3094$, $b = -0.0028$	0.9982	0.0141	0.000286
50°C (U-20)	Logarithmic	$a = 1.1807$, $k = 0.1824$, $c = -0.1773$	0.9989	0.0106	0.000149
50°C (U-40)	Midilli et al. [30]	$a = 0.9745$, $k = 0.1277$, $n = 1.3548$, $b = -0.0027$	0.9948	0.0236	0.000803
60°C – control	Midilli et al. [30]	$a = 0.9913$, $k = 0.1637$, $n = 1.5579$, $b = -0.0017$	0.9993	0.00903	0.000136
60°C (U-20)	Midilli et al. [30]	$a = 0.9926$, $k = 0.1721$, $n = 1.3752$, $b = -0.0065$	0.9942	0.0264	0.00117
60°C (U-40)	Midilli et al. [30]	$a = 1.0017$, $k = 0.1830$, $n = 1.3183$, $b = -0.0057$	0.9984	0.0137	0.000312

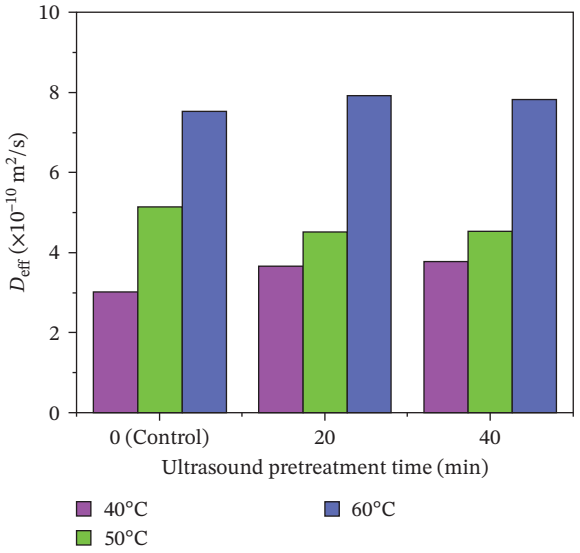


FIGURE 2 | Effective moisture diffusivity of tomato slices as influenced by drying temperature (40, 50, and 60°C) and ultrasound pretreatment time (0, 20, and 40 min).

with temperature and that moderate ultrasound pretreatment (20 min) enhances internal water diffusion at lower drying intensities without the risk of overprocessing associated with prolonged exposure. Similar temperature- and ultrasound-dependent trends have been reported for other agricultural materials. Salehi [51] reported that the average D_{eff} increased from 1.36×10^{-10} to 1.88×10^{-10} m^2/s when ultrasound pretreatment was extended from 0 min (control) to 20 min for sprouted mung beans dried in a hot-air dryer. Jahanbakhshi et al. [17] observed D_{eff} values ranging from 6.50×10^{-10} m^2/s in untreated nectarine slices dried at 50°C to 2.11×10^{-9} m^2/s in samples pretreated with ultrasound for 40 min and dried at 75°C. Variations in reported D_{eff} values across agricultural products might be due to the different drying temperatures, moisture content, and applied pretreatment conditions.

3.4 | Activation Energy of Moisture Diffusion

Activation energy (E_a) reflects the minimum energy required for moisture molecules to overcome internal resistance and diffuse through the matrix [24]. In this study, E_a values for tomato slices dried between 40–60°C were 39.86 kJ/mol for the control, 33.28 kJ/mol for U-20, and 31.28 kJ/mol for U-40 (Table 3). The consistent decrease in E_a with ultrasound pretreatment indicates that ultrasonication facilitates moisture transport by lowering the diffusion energy barrier [52, 53]. Although U-40 yielded the numerically lowest E_a, the small difference from U-20 (2 kJ/mol) is likely within the uncertainty of the Arrhenius fits.

Importantly, E_a alone does not dictate the drying rate; both E_a and the pre-exponential factor (D_0) jointly govern diffusional transport. Prolonged sonication may reduce E_a by lowering temperature sensitivity while simultaneously decreasing D_0, suggesting that less thermal energy is needed to sustain moisture removal but that structural over-disruption may offset kinetic gains. Hence, while a lower E_a generally corresponds to enhanced diffusion efficiency, excessive ultrasonication (U-40) could compromise quality attributes such as texture, rehydration, or color stability. Thus, U-20 represents an optimal balance, achieving a substantially lower E_a than the control without risking overprocessing effects. Similar findings were reported in the literature. Yamchi et al. [18] observed a reduction in E_a from 41.43 to 36.74 kJ/mol in ripe and from 42.91 to 37.49 kJ/mol in unripe bitter melon slices pretreated for 20 min, confirming that moderate ultrasound exposure improves diffusional energetics without requiring extreme temperature or pretreatment conditions.

3.5 | Thermodynamic Parameters of the Drying Process

Table 4 shows the thermodynamic activation parameters ($\Delta H^{\dagger}$, $\Delta S^{\dagger}$, and $\Delta G^{\dagger}$) describing moisture diffusion in control and ultrasonicated tomato slices at different drying temperatures. $\Delta H^{\dagger}$ represents the energy barrier for molecular diffusion, while $\Delta S^{\dagger}$

TABLE 3 | Activation energy in tomato slices as influenced by ultrasound pretreatment.

Treatment	E_a (kJ/mol)	D_0 (m^2/s)	R^2
0 (control)	39.86	0.00137	0.9937
U-20	33.28	0.000123	0.9275
U-40	31.28	0.0000589	0.9127

TABLE 4 | Thermodynamic activation parameters for moisture diffusion in tomato slices as influenced by ultrasound pretreatment and drying temperature.

Treatment	T (°C)	$\Delta H^{\dagger}$ (kJ/mol)	$\Delta S^{\dagger}$ (J/mol.K)	$\Delta G^{\dagger}$ (kJ/mol)
0 (control)	40	39.53	−283.03	311.57
	50	39.45	−284.89	321.18
	60	39.36	−286.40	330.79
U-20	40	32.95	−303.07	311.83
	50	32.87	−304.92	321.51
	60	32.79	−306.44	331.18
U-40	40	30.95	−309.20	311.91
	50	30.87	−311.05	321.61
	60	30.79	−312.57	331.30

and $\Delta G^{\dagger}$ describe the degree of molecular ordering and overall energetic feasibility, respectively. In all treatments, $\Delta H^{\dagger}$ and $\Delta S^{\dagger}$ decreased with increasing temperature, whereas $\Delta G^{\dagger}$ increased, consistent with trends reported for other agricultural materials [54, 55]. The decrease in $\Delta H^{\dagger}$ with ultrasound pretreatment confirms that sonication lowers the energetic barrier to diffusion, thereby enhancing moisture mobility. The additional reduction in $\Delta H^{\dagger}$ from U-20 (32.95–32.79 kJ/mol across 40–60°C) to U-40 (30.95–30.79 kJ/mol) was consistently 2.00 kJ/mol at each temperature, suggesting diminishing returns beyond moderate treatment intensity [42, 52].

All $\Delta S^{\dagger}$ values were negative, indicating an ordered transition state typical of food drying, where water molecules become transiently restricted at cell interfaces before diffusion [55]. The more negative $\Delta S^{\dagger}$ in ultrasonicated samples suggests increased ordering in the transition complex, likely due to microchannel formation and localized structural compaction induced by acoustic cavitation. This is consistent with the observed reductions in shrinkage and the shift in the dominant drying model structure under ultrasound-treated conditions.

Positive $\Delta G^{\dagger}$ values across all conditions indicate that moisture diffusion requires external energy input, consistent with the nonspontaneous nature of drying processes [56]. The increase in $\Delta G^{\dagger}$ with temperature arises from the compensating effect of the negative $\Delta S^{\dagger}$ term, which raises the free-energy barrier at higher intensities. These findings show that ultrasound pretreatment reduces the enthalpic barrier while increasing the transition-state order. Although U-40 yielded slightly lower $\Delta H^{\dagger}$, the concurrent strong decrease in $\Delta S^{\dagger}$ implies greater structural tightening. Thus, U-20 represents a more balanced condition, achieving improved energy efficiency without risking excessive tissue alteration.

3.6 | Total Specific Energy Consumption During Drying

Energy consumption is a critical indicator of drying efficiency, reflecting both process performance and sustainability. The total specific energy consumption (E_T) quantifies the energy required to remove 1 kg of water, serving as a benchmark for process optimization [57]. As shown in Figure 3, E_T decreased with increasing drying temperature, with control samples recording 195.99, 186.46, and 133.98 kWh/kg at 40°C, 50°C, and 60°C, respectively. This reduction aligns with the well-established principle that higher temperatures accelerate moisture removal, shorten drying time, and, thereby, reduce the total energy input per unit of water evaporated [17, 24, 58].

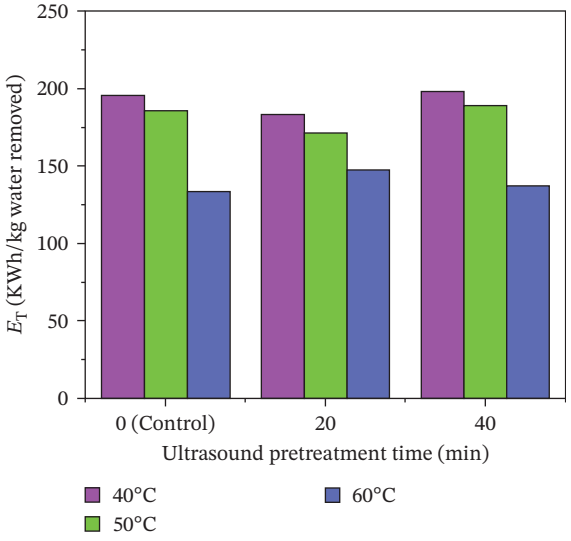


FIGURE 3 | Total specific energy consumption during hot-air drying of tomato slices as influenced by drying temperature and ultrasound pretreatment time.

Ultrasonic pretreatment further influenced E_T. Moderate sonication (U-20) lowered energy consumption to 183.55, 171.63, and 148.07 kWh/kg at 40°C, 50°C, and 60°C, respectively, showing the most significant saving at lower temperatures. In contrast, prolonged sonication (U-40) produced higher E_T values (198.21, 189.61, and 137.77 kWh/kg) at 40 and 50°C compared to both the control and U-20 treatments. This behavior can be explained by the fact that U-40 did not reduce drying time relative to the control at these temperatures, indicating that the increased pretreatment intensity did not translate into improved moisture removal during drying. This observation is consistent with the structural over-disruption hypothesis, whereby excessive cavitation may collapse cellular capillaries and disrupt internal moisture transport pathways, thereby negating the kinetic advantages of ultrasonication and resulting in a higher overall energy demand. A similar dependence of energy efficiency on ultrasound pretreatment intensity has also been reported by Yamchi et al. [18]. However, at 60°C, both ultrasound treatments reduced E_T, reflecting the dominant influence of rapid moisture diffusion under stronger thermal driving forces. These findings demonstrate that the energy efficiency of ultrasound-assisted drying is strongly dependent on pretreatment duration and that moderate sonication (U-20) provides the most favorable balance between enhanced drying kinetics and reduced energy consumption. The E_T values obtained in this study (133.98–198.21 kWh/kg) are consistent with the range of 59.70–212.97 kWh/kg reported by Jahanbakhshi et al. [17] for hot-air drying of ultrasound-pretreated nectarine slices, confirming that hot-air drying remains relatively energy-intensive compared to hybrid technologies. In this regard, Abbaspour-Gilandeh et al. [39] reported that ultrasound pretreatment reduced specific energy consumption by 13.2%–67.4% in infrared drying of

cantaloupe slices, highlighting the potential of combining ultrasound pretreatment with lower energy drying technologies to achieve greater energy savings than hot-air drying alone can provide. Beyond ultrasound, other structural pretreatments have demonstrated similar energy-saving potential; for instance, vacuum-steam pulsed blanching reduced specific energy consumption by up to 40% at 70°C during hot-air drying of *Vigna unguiculata pods* [59], further underscoring that pretreatment-induced structural modifications broadly enhance drying energy efficiency regardless of the pretreatment type.

3.7 | Quality Attributes

3.7.1 | Color Changes During Drying

Color is a critical sensory attribute of dried foods and an indicator of both visual and nutritional quality [60, 61]. In this study, the total color difference (ΔE) of tomato slices varied with the drying temperature and ultrasound pretreatment (Figure 4). For control samples, ΔE values were 9.92 ± 1.05 at 40°C to 20.28 ± 1.33 at 50°C and then declined to 13.67 ± 1.07 at 60°C, reflecting a nonlinear relationship between temperature and color degradation. The peak ΔE at 50°C likely resulted from the longer drying time at this intermediate temperature, which promoted Maillard browning and carotenoid isomerization, whereas the shorter exposure at 60°C limited these reactions [62].

Ultrasonic pretreatment significantly influenced color retention. Moderate exposure (U-20) reduced ΔE across all temperatures, most notably to 6.75 ± 1.52 at 60°C, indicating improved pigment preservation through enhanced water diffusion and shorter drying times. Conversely, prolonged sonication (U-40) markedly increased ΔE (up to 26.05 ± 1.16 at 40°C), suggesting that excessive treatment caused cellular damage and oxidative degradation of pigments.

ΔE depended on both temperature and ultrasound duration: moderate treatment (U-20) improved color retention, while overexposure (U-40) intensified browning. Across all treatments, the minimum ΔE (best color retention) occurred at 60°C (U-20) and the maximum at 40°C (U-40). Comparable findings have been reported for other crops. Zhang et al. [63] observed that applying a 250 W ultrasound for 5 min before drying ginger slices resulted in a minimum discoloration value of 8.665. Yamchi et al. [64] reported that ΔE values in peach slices decreased with ultrasound pretreatment, with the minimum at 9.96% for 60 min of sonication compared to a maximum of 12.89% in the control. Similarly, Jahanbakhshi et al. [17] found that increasing ultrasound pretreatment time reduced the total color change in nectarine slices, with the lowest ΔE reported as 15.87%. These results confirm that combining higher drying temperatures with moderate ultrasound pretreatment is optimal for maintaining the natural color and consumer appeal of dried tomato slices.

3.7.2 | Changes in TPC

Phenolic compounds are important bioactive molecules with antioxidant properties whose retention indicates the nutritional quality of dried foods. In this study, the TPC of fresh tomato slices was 9.73 ± 0.39 mg GAE/g DW. Drying at 40°C reduced TPC below the fresh value across all treatments, with the control recording 3.90 ± 0.11 mg GAE/g DW, likely due to the prolonged drying time and associated oxidative degradation. However, TPC increased with drying temperature across all treatments (Figure 5). In the control, TPC increased from 3.90 ± 0.11 mg GAE/g DW at 40°C to 8.65 ± 0.35 mg GAE/g DW at 50°C and 14.43 ± 0.43 mg GAE/g DW at 60°C, with the value at 60°C exceeding that of the fresh sample. This pattern suggests that although mild drying conditions may promote phenolic degradation, higher temperatures may enhance phenolic extractability through faster moisture removal, heat-induced cell-wall disruption, and inactivation of oxidative enzymes such as polyphenol oxidase and peroxidase [65, 66].

Ultrasonic pretreatment influenced TPC in a time- and temperature-dependent manner. At 40°C, U-20 slightly increased TPC to 4.21 ± 0.25 mg GAE/g DW compared with the control (3.90 ± 0.11 mg GAE/g DW), suggesting a modest benefit of moderate

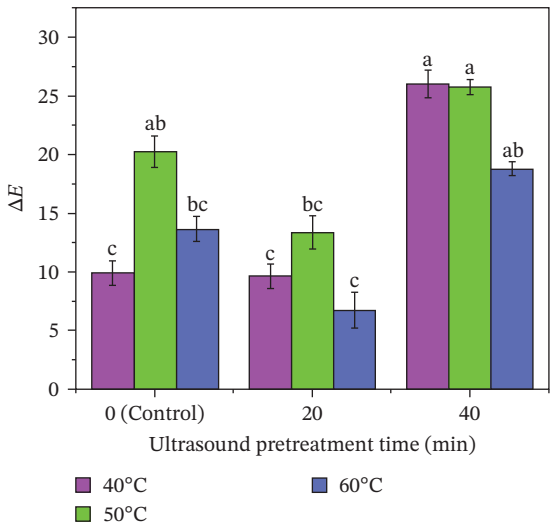


FIGURE 4 | Total color difference of dried tomato slices as influenced by drying temperature (40, 50, and 60°C) and ultrasound pretreatment time (0, 20, and 40 min). Error bars with difference lower case letters are significantly different ($p < 0.05$).

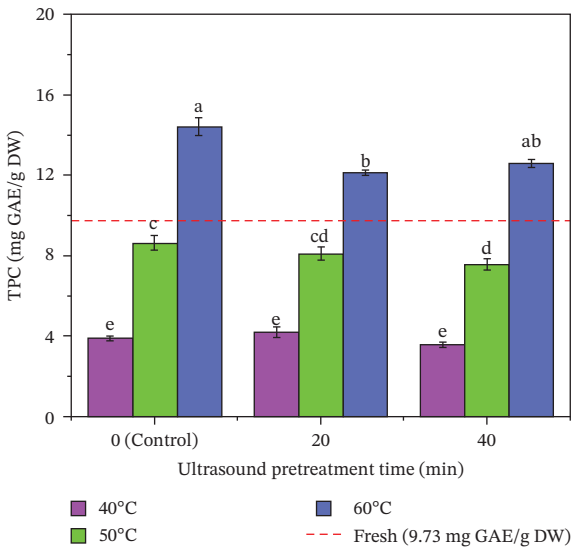


FIGURE 5 | Total phenolic content of fresh and dried tomato slices as influenced by drying temperature and ultrasound pretreatment time. Error bars with difference lower case letters are significantly different ($p < 0.05$).

sonication under mild drying conditions. However, at 50 and 60°C, both ultrasound treatments produced lower TPC than the control, with U-20 recording 8.12 ± 0.32 and 12.14 ± 0.14 mg GAE/g DW and U-40 recording 7.59 ± 0.28 and 12.60 ± 0.19 mg GAE/g DW at 50°C and 60°C, respectively. These reductions may reflect the leaching of soluble phenolic compounds into the immersion medium during ultrasound pretreatment and/or oxidative changes associated with cavitation-induced tissue disruption [65, 66]. The highest TPC was recorded in the control at 60°C (14.43 ± 0.43 mg GAE/g DW), which was ~ 48% higher than the fresh sample, while the lowest was observed in the U-40 sample at 40°C (3.59 ± 0.11 mg GAE/g DW). Thus, increasing drying temperature enhanced extractable TPC, while ultrasound pretreatment showed only a limited advantage at 40°C and tended to reduce TPC relative to the control at higher temperatures.

3.7.3 | Shrinkage Behavior of Tomato Slices

Shrinkage reflects the extent of structural collapse and porosity loss during drying, directly influencing the texture, bulk density, and rehydration ability. As shown in Figure 6a, volumetric shrinkage of tomato slices increased with temperature from 41.76 ± 0.55% at 40°C to 46.15 ± 1.10% at 60°C in the control samples. This progressive increase results from accelerated moisture removal and internal stress at higher temperatures, which intensify structural collapse.

Ultrasound pretreatment reduced shrinkage across all temperatures, with U-20 reducing shrinkage by 0.83%–2.74% and U-40 by 1.38–3.29% relative to the control, with the greatest reductions observed at 60°C. This confirms that ultrasound moderates thermal stress and maintains structural integrity. Although U-40 achieved marginally greater shrinkage reductions than U-20, this likely reflects excessive tissue disruption rather than improved structural preservation, as over-sonication compromises cell-wall integrity and accelerates collapse under thermal stress. U-20, therefore, represents a more structurally sound outcome, achieving meaningful shrinkage reduction without the risks associated with prolonged cavitation. Our findings align with those in previous reports. Jahanbakhshi et al. [17] reported reduced shrinkage in ultrasonicated nectarine slices compared to controls during hot-air drying at 50–75°C. Yamchi et al. [18] found that the shrinkage of both ripe and unripe bitter melon increased with drying temperature but decreased with ultrasound pretreatment, with the lowest values recorded in U-20 samples dried at 50°C. These results indicate that temperature is the primary factor driving shrinkage, whereas ultrasound pretreatment, especially at moderate duration, mitigates structural damage, supporting better physical and functional quality of the dried product.

3.7.4 | RR of Dried Tomato Slices

The RR indicates the extent of structural integrity retained after drying and thus reflects the ability of the material to absorb water upon rehydration [39]. As shown in Figure 6b, RR decreased with increasing drying temperature from 4.67 ± 0.11 at 40°C to 4.02 ± 0.28 at 60°C for control samples. This decline reflects progressive cell-wall hardening and pore collapse at higher thermal intensities, which restricts the water uptake.

Ultrasonic pretreatment influenced RR in a temperature-dependent manner. At 40°C, sonication lowered RR from 4.67 ± 0.11 (control) to 4.37 ± 0.01 (U-20) and 4.23 ± 0.14 (U-40) due to additional tissue disruption under mild drying conditions. However, at 50–60°C, ultrasound produced slightly higher RR values than the control, with U-20 and U-40 reaching 4.39 and 4.49 at 50°C and 4.18 and 4.23 at 60°C, respectively, compared with control values of 4.37 and 4.02. This suggests that microchannel formation mitigated structural collapse and preserved permeability at severe thermal regimes. Across all treatments, the highest RR occurred in the control at 40°C, while the lowest was observed in the control at 60°C, consistent with greater case hardening and cross-linking at high temperatures.

Higher RR values signify better structural preservation and reconstitution quality. The most favorable conditions for RR were observed at 40–50°C, where moderate ultrasound exposure

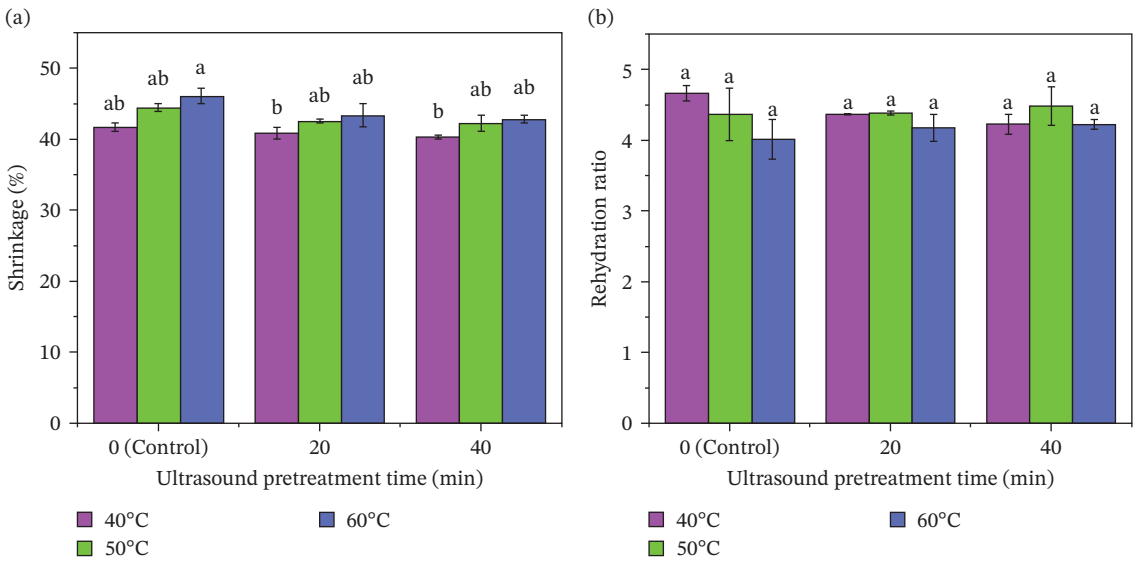


FIGURE 6 | Effect of drying temperature (40, 50, and 60°C) and ultrasound pretreatment time (0, 20, and 40 min) on: (a) shrinkage and (b) rehydration ratio of dried tomato slices.

improved the rehydration performance. Similar findings have been reported for other plant materials. Salehi [51] observed that the RR of sprouted mung beans dried in a hot-air dryer at 50°C increased when 20 min of ultrasound pretreatment was applied compared with untreated samples. Yamchi et al. [18] found the highest RR for ripe and unripe bitter melon with 20 min ultrasound and 70°C drying and rehydration at 65°C; the lowest RR in their work was for controls dried at 50°C and rehydrated at 25°C. These studies support our conclusion that temperature primarily governs rehydration behavior, while ultrasound can alleviate drying-induced damage and sustain water-absorption capacity under high-temperature conditions.

3.7.5 | Pearson's Correlation Analysis

Pearson's correlation analysis (Figure 7) revealed that both temperature and ultrasonication primarily influenced tomato-slice quality through their impact on moisture removal. For TPC, temperature correlated positively ($r = 0.672$, $p < 0.05$), indicating that faster water removal, which disrupted cell walls and released bound compounds, enhanced phenolic extractability. Ultrasonication, however, correlated negatively ($r = -0.49$), suggesting that extended cavitation exposure may have induced the oxidation or degradation of phenolics. Thus, temperature promoted diffusion-driven release, while prolonged ultrasonication limited phenolic stability. In terms of color, ultrasonication showed a positive linear correlation with color change ($r = 0.548$), though this reflects a nonlinear underlying relationship. Moderate pretreatment (20 min) markedly reduced color change, while prolonged exposure (40 min) increased it substantially, indicating that the beneficial effect of ultrasonication on color retention is duration-dependent and is not adequately captured by a simple linear association. Temperature showed a weak negative correlation ($r = -0.131$), suggesting a minimal independent influence on color change across the range studied.

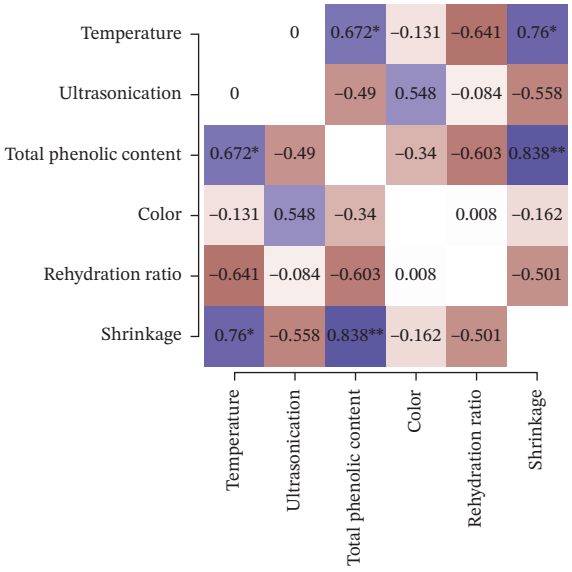


FIGURE 7 | Pearson's correlation heatmap illustrating the relationships between drying parameters and quality attributes of tomato slices. The color scale represents the Pearson correlation coefficient (r), ranging from –1 (strong negative correlation, red) to +1 (strong positive correlation, blue), with color intensity indicating the strength of the relationship and white indicating no correlation ($r \approx 0$). Correlation coefficients are displayed within each cell; * and ** denote statistical significance at $p < 0.05$ and $p < 0.01$, respectively.

For the RR, both factors showed negative correlations: temperature ($r = -0.641$) and ultrasonication ($r = -0.084$), indicating that faster moisture loss and tissue collapse at higher energy inputs lowered the ability of the dried tomato slices to reabsorb water. Shrinkage increased with temperature ($r = 0.76$, $p < 0.05$) but decreased with ultrasonication ($r = -0.558$). Rapid evaporation caused by heat promoted structural contraction, while ultrasound-assisted diffusion reduced surface hardening and helped retain the structure. Thus, the correlations confirm that temperature mainly governs the rate of evaporation, whereas ultrasonication modifies moisture diffusion. An optimal combination of moderate temperature and short ultrasonication ensures efficient drying with minimal quality deterioration.

4 | Conclusion

This study demonstrated that ultrasound pretreatment combined with hot-air drying significantly improved the drying efficiency and product quality of tomato slices. Among the conditions evaluated, 20 min of ultrasound pretreatment produced the most balanced outcome, enhancing moisture transport, lowering the energy barrier for diffusion, and preserving structural and visual quality. Prolonged sonication (40 min) offered no additional kinetic benefit and, in some cases, caused adverse color and textural effects. The drying behavior was best described by the Midilli–Kucuk et al.'s thin-layer model, confirming its suitability for ultrasound-assisted drying systems. Thermodynamic analysis showed that ultrasound reduced the enthalpic requirement and promoted molecular ordering, indicating a more favorable moisture diffusion pathway. Total specific energy consumption decreased with increasing temperature, and 20 min pretreatment achieved the greatest energy savings across the full temperature range, particularly under mild drying conditions. Although 40 min of sonication yielded marginally lower energy consumption at 60°C, this advantage was outweighed by its adverse quality effects, making 20 min of pretreatment the more consistently efficient and quality-preserving choice. From a quality standpoint, 20 min pretreatment reduced shrinkage while maintaining structural integrity, enhanced rehydration capacity, and best-preserved color. Based on the combined evaluation of drying kinetics, thermodynamic behavior, energy consumption, and product quality, the combination of 20 min of ultrasound pretreatment followed by hot-air drying at 60°C is recommended as the optimal condition for maximizing drying efficiency and color retention, while 40–50°C may be preferable when rehydration capacity is prioritized. Future research should investigate the scalability of ultrasound-assisted drying under continuous processing conditions, optimize pretreatment parameters for different tomato cultivars and slice thicknesses, and explore hybrid drying strategies to further improve the energy efficiency and product quality.

Author Contributions

Eyitayo Kehinde Oladipo: conceptualization, methodology, investigation, formal analysis, data curation, writing – original draft. **Zinash A.**

Belay: supervision, visualization, writing – review and editing, resources, methodology. **Oluwafemi James Caleb**: conceptualization, supervision, validation, writing – review and editing, funding acquisition, resources.

Acknowledgments

This work is based upon research supported wholly/in part by the Technology Innovation Agency, South Africa, and the Academy for Scientific Research and Technology, Egypt (Grant 2024/FUN293/AA) awarded to Dr. Caleb. The PhD scholarship awarded to EK Oladipo by the Postharvest BioSystems Consultation Programme is gratefully acknowledged.

Funding

This research was supported by the Technology Innovation Agency, South Africa (Grant 2024/FUN293/AA) and the Academy for Scientific Research and Technology, Egypt (Grant 2024/FUN293/AA).

Conflicts of Interest

The authors declare no conflicts of interest.

Data Availability Statement

The data that support the findings of this study are available from the corresponding author upon reasonable request.

References

1. E. K. Oladipo, B. Oladipo, T. V. Ojumu, and O. J. Caleb, "Postharvest Losses of Tomato: Causes, Spoilage Mechanisms, and Advances in Conventional and Emerging Technologies for Preservation," *Food Research International* 227 (2026): 118247.

2. A. Rai, K. Kumari, and P. Vashistha, "Umbrella Review on Chilling Injuries: Post-Harvest Issue, Cause, and Treatment in Tomato," *Scientia Horticulturae* 293 (2022): 110710.

3. K. Jayaraman and D. D. Gupta, "Drying of Fruits and Vegetables," in *Handbook of Industrial Drying*, (CRC Press, 2020): 643–690.

4. M. U. Hasan, A. U. Malik, S. Ali, et al., "Modern Drying Techniques in Fruits and Vegetables to Overcome Postharvest Losses: A Review," *Journal of Food Processing and Preservation* 43, no. 12 (2019).

5. F. Fathi, S. N. Ebrahimi, L. C. Matos, M. B. P. P. Oliveira, and R. C. Alves, "Emerging Drying Techniques for Food Safety and Quality: A Review," *Comprehensive Reviews in Food Science and Food Safety* 21, no. 2 (2022): 1125–1160.

6. N. S. Bhatkar, S. S. Shirkole, A. S. Mujumdar, and B. N. Thorat, "Drying of Tomatoes and Tomato Processing Waste: A Critical Review of the Quality Aspects," *Drying Technology* 39, no. 11 (2021): 1720–1744.

7. M. Pravitha, M. Dipika Agrahar, and V. Ajesh Kumar, "Recent Developments in Tomato Drying Techniques: A Comprehensive Review," *Journal of Food Process Engineering* 47, no. 2 (2024).

8. L.-S. Cheng, S. Fang, and M.-L. Ruan, "Influence of Blanching Pretreatment on the Drying Characteristics of Cherry Tomato and Mathematical Modeling," *International Journal of Food Engineering* 11, no. 2 (2015): 265–274.

9. E. K. Dermesonlouoglou, K. Pantelaiaki, V. Andreou, G. J. Katsaros, and P. S. Taoukis, "Osmotic Pretreatment for the Production of Novel Dehydrated Tomatoes and Cucumbers," *Journal of Food Processing and Preservation* 43, no. 7 (2019).

10. L.-Z. Deng, A. S. Mujumdar, Q. Zhang, et al., "Chemical and Physical Pretreatments of Fruits and Vegetables: Effects on Drying Characteristics and Quality Attributes–a Comprehensive Review," *Critical Reviews in Food Science and Nutrition* 59, no. 9 (2019): 1408–1432.

11. M. O. Sunmonu, M. Odewole, E. Ajala, R. Sani, and A. Ogunbiyi, "Effect of Two Blanching Methods on the Nutritional Values of Tomatoes and Pumpkin Leaves," *Journal of Applied Sciences and Environmental Management* 25, no. 2 (2021): 183–187.

12. S. Zhou, W. Chen, B. Chitrakar, and K. Fan, "Ultrasound Technology for Enhancing Drying Efficiency and Quality of Fruits and Vegetables: A Review," *Food and Bioprocess Technology* 17, no. 12 (2024): 4506–4536.

13. K. Fan, J. Wu, and L. Chen, "Ultrasound and Its Combined Application in the Improvement of Microbial and Physicochemical Quality of Fruits and Vegetables: A Review," *Ultrasonics Sonochemistry* 80 (2021): 105838.

14. D. Fotiou, K. Argyropoulos, P. Kolompourda, and A. M. Goula, "Valorization of Peach Peels: Preservation with an Optimized Drying Process Based on Ultrasounds Pretreatment with Ethanol," *Biomass Conversion and Biorefinery* 13, no. 18 (2023): 16345–16357.

15. X. Cao, M. N. Islam, S. Zhong, et al., "Drying Kinetics, Antioxidants, and Physicochemical Properties of Litchi Fruits by Ultrasound-Assisted Hot Air-Drying," *Journal of Food Biochemistry* 44, no. 1 (2019).

16. M. Feng, B. Xu, M. N. Islam, et al., "Individual and Synergistic Effect of Multi-Frequency Ultrasound and Electro-Infrared Pretreatments on Polyphenol Accumulation and Drying Characteristics of Edible Roses," *Food Research International* 163 (2023): 112120.

17. A. Jahanbakhshi, R. Yeganeh, and M. Momeny, "Influence of Ultrasound Pre-Treatment and Temperature on the Quality and Thermodynamic Properties in the Drying Process of Nectarine Slices in a Hot Air Dryer," *Journal of Food Processing and Preservation* 44, no. 10 (2020).

18. A. A. Yamchi, A. Hosainpour, A. Hassanpour, and A. R. Fanaei, "Drying Kinetics and Thermodynamic Properties of Ultrasound Pretreatment Bitter Melon Dried by Infrared," *Journal of Food Processing and Preservation* 2024, no. 1 (2024): 1987547.

19. J. Wang, H.-W. Xiao, J.-H. Ye, J. Wang, and V. Raghavan, "Ultrasound Pretreatment to Enhance Drying Kinetics of Kiwifruit (*Actinidia Deliciosa*) Slices: Pros and Cons," *Food and Bioprocess Technology* 12, no. 5 (2019): 865–876.

20. L.-V. E. César, C.-M. A. Lilia, G.-V. Octavio, P. F. Isaac, and B. O. Rogelio, "Thermal Performance of a Passive, Mixed-Type Solar Dryer for Tomato Slices (*Solanum lycopersicum*)," *Renewable Energy* 147 (2020): 845–855.

21. O. I. Obajemihi, O. J. Esua, J.-H. Cheng, and D.-W. Sun, "Effects of Pretreatments Using Plasma Functionalized Water, Osmodehydration and Their Combination on Hot Air Drying Efficiency and Quality of Tomato (*Solanum lycopersicum* L.) Slices," *Food Chemistry* 406 (2023): 134995.

22. S. Guemouni, K. Mouhoubi, F. Brahmi, et al., "Convective and Microwave Drying Kinetics and Modeling of Tomato Slices, Energy Consumption, and Efficiency," *Journal of Food Process Engineering* 45, no. 9 (2022).

23. S. Tan, Y. Miao, H. Xiang, W. Tan, and W. Li, "Effects of Air-Impingement Jet Drying on Drying Kinetics and Quality Retention of Tomato Slices," *Food Science and Biotechnology* 30, no. 5 (2021): 691–699.

24. O. O. Agbede, E. O. Oke, S. I. Akinfenwa, et al., "Thin Layer Drying of Green Microalgae (Chlorella sp.) Paste Biomass: Drying Characteristics, Energy Requirement and Mathematical Modeling," *Bioresource Technology Reports* 11 (2020): 100467.

25. B. T. Olawoye, O. Kadiri, and T. R. Babalola, "Modelling of Thin-Layer Drying Characteristic of Unripe Cardaba Banana (*Musa* ABB) Slices," *Cogent Food & Agriculture* 3, no. 1 (2017): 1290013.

26. W. K. Lewis, "The Rate of Drying of Solid Materials," *Journal of Industrial & Engineering Chemistry* 13, no. 5 (1921): 427–432.

27. G. E. Page, *Factors Influencing the Maximum Rates of Air Drying Shelled Corn in Thin Layers* Purdue University, 1949).

28. S. Henderson, "Grain Drying Theory (I) Temperature Effect on Drying Coefficient," *Journal of Agricultural Engineering Research* 6, no. 3 (1961): 169–174.

29. P. K. Chandra and R. P. Singh, *Applied Numerical Methods for Food and Agricultural Engineers* (CRC Press, 2017).

30. A. Midilli, H. Kucuk, and Z. Yapar, "A New Model for Single-Layer Drying," *Drying Technology* 20, no. 7 (2007): 1503–1513.

31. L. R. Verma, R. Bucklin, J. Endan, and F. Wratten, "Effects of Drying Air Parameters on Rice Drying Models," *Transactions of the ASAE* 28, no. 1 (1985): 296–301.

32. W. Wang, J. Chen, N. Jin, H. Wang, L. Wang, and J. Wu, "Thin-Layer Drying Model, Drying Rate, and Effective Water Diffusion Coefficient of Pelleted Feed," *International Journal of Chemical Engineering* 2024, no. 1 (2024).

33. A. R. Celma, S. Rojas, and F. Lopez-Rodriguez, "Mathematical Modelling of Thin-Layer Infrared Drying of Wet Olive Husk," *Chemical Engineering and Processing: Process Intensification* 47, no. 9-10 (2008): 1810–1818.

34. J. Crank, *The Mathematics of Diffusion* (Clarendon Press).

35. K. Di Scala and G. Crapiste, "Drying Kinetics and Quality Changes During Drying of Red Pepper," *LWT-Food Science and Technology* 41, no. 5 (2008): 789–795.

36. A. Vega-Gálvez, M. Miranda, L. P. Díaz, L. Lopez, K. Rodriguez, and K. Di Scala, "Effective Moisture Diffusivity Determination and Mathematical Modelling of the Drying Curves of the Olive-Waste Cake," *Bioresource Technology* 101, no. 19 (2010): 7265–7270.

37. E.-S. G. Khater, A. H. Bahnasawy, A. E. Elwakeel, et al., "Comparative Analysis of Drying Kinetics, Thermodynamic Properties, and Mathematical Modeling of Pomegranate Peel (*Punica granatum* L.) in a Hybrid Solar Dryer and an Oven Dryer," *Scientific Reports* 15, no. 1 (2025).

38. M. E. Cavalcanti-Mata, M. E. Duarte, M. Tolentino, et al., "Drying Kinetics of Industrial Pineapple Waste: Effective Diffusivity and Thermodynamic Properties Resulting From New Mathematical Models Derived From the Fick Equation," *Processes* 12, no. 6 (2024): 1198.

39. Y. Abbaspour-Gilandeh, M. Kaveh, S. Zadhossein, B. Gheisary, and H. S. El-Mesery, "Application of Ultrasound Treatment in Cantaloupe Infrared Drying Process: Effects on Moisture Migration and Microstructure," *Journal of Food Science* 90, no. 3 (2025).

40. L. A. Yanclo, G. Sigge, Z. A. Belay, A. B. Oyenihi, and O. J. Caleb, "Evaluation of Low-Pressure Cold Plasma Effect on Phytonutrients," in *Drying and Microstructural Characteristics, and Changes in Microbial Load of Fresh and Hot-Air-Dried* (2024): 1–19

41. M. D. E. M. Rosdan, M. A. Awang, M. A. Z. Benjamin, S. F. Mohd Amin, and N. Julmohammad, "Effect of Ultrasound-Assisted Osmotic Dehydration (UAOD) Pretreatment on, *Mangifera pajang*, Kosterm. Fruit Pulp: Drying Kinetics, Chemical Qualities, and Color Measurement," *Journal of Food Process Engineering* 47, no. 9 (2024).

42. R. Pandiselvam, A. Y. Aydar, N. Kutlu, et al., "Individual and Interactive Effect of Ultrasound Pre-Treatment on Drying Kinetics and Biochemical Qualities of Food: A Critical Review," *Ultrasonics Sonochemistry* 92 (2023): 106261.

43. T. Alvi, M. K. I. Khan, A. A. Maan, et al., "Microwave–vacuum Extraction Cum Drying of Tomato Slices: Optimization and Functional Characterization," *Food Science & Nutrition* 11, no. 7 (2023): 4263–4274.

44. W. S. Ribeiro, A. S. Silva, Á.G. F. da Silva, et al., "Handmade Solar Dryer: An Environmentally and Economically Viable Alternative for Small and Medium Producers," *Scientific Reports* 11, no. 1 (2021).

45. D. I. Onwude, N. Hashim, R. B. Janius, N. M. Nawi, and K. Abdan, "Modeling the Thin-Layer Drying of Fruits and Vegetables: A Review," *Comprehensive Reviews in Food Science and Food Safety* 15, no. 3 (2016): 599–618.

46. A. Dönmez and Ç. Kadakal, "Hot-Air Drying and Degradation Kinetics Of Bioactive Compounds Of Gilaburu (*Viburnum opulus* L.) Fruit," *Chemical Industry and Chemical Engineering Quarterly* 30, no. 1 (2024): 59–72.

47. M. Manikantan, D. Mridula, M. Sharma, et al., "Investigation on Thin-Layer Drying Kinetics of Sprouted Wheat in a Tray Dryer," *Quality Assurance and Safety of Crops and Foods* 14, no. SP1 (2022): 12–24.

48. B. Llavata, A. Femenia, G. Clemente, and J. Cárcel, "Combined Effect of Airborne Ultrasound and Temperature on the Drying Kinetics and Quality Properties of Kiwifruit (*Actinidia Deliciosa*)," *Food and Bioprocess Technology* 17, no. 2 (2024): 440–451.

49. T. T. H. Tran, T. T. D. Nguyen, A. Kharaghani, and K. H. Le, "The Impact of Ultrasound Pre-Treatment on Hot-Air-Drying Kinetics and Quality of Carrot Slices Assessed by Simulations and Experiments," *Applied Sciences* 13, no. 21 (2023): 11865.

50. Z. Erbay and F. Icier, "A Review of Thin Layer Drying of Foods: Theory, Modeling, and Experimental Results," *Critical Reviews in Food Science and Nutrition* 50, no. 5 (2010): 441–464.

51. F. Salehi, "Effects of Ultrasonic Pretreatment and Drying Approaches on the Drying Kinetics and Rehydration of Sprouted Mung Beans," *Legume Science* 5, no. 4 (2023).

52. N. C. Santos, R. L. J. Almeida, G. M. da Silva, S. S. Monteiro, and A. M. M. Andre, "Effect of Ultrasound Pre-Treatment on the Kinetics and Thermodynamic Properties of Guava Slices Drying Process," *Innovative Food Science & Emerging Technologies* 66 (2020): 102507.

53. A. Niveditha, D. Chidanand, and C. Sunil, "Effect of Ultrasound-Assisted Drying on Drying Kinetics, Color, Total Phenols Content and Antioxidant Activity of Pomegranate Peel," *Measurement: Food* 12 (2023): 100114.

54. Y. B. Öztekin, M. Aktaş, E. C. Dolgun, H. C. Bilim, and K. Sacilik, "Drying Kinetics and Thermodynamic Properties of Uzun Pistachios Dried by Convective Drying," *Journal of Food Processing and Preservation* 46, no. 11 (2022).

55. H. V. Moura, R. M. F. de Figueirêdo, A. J. de Melo Queiroz, E. T. de Vilela Silva, J. A. D. Esmero, and J. F. Lisbôa, "Mathematical Modeling and Thermodynamic Properties of the Drying Kinetics of Trapiá Residues," *Journal of Food Process Engineering* 44, no. 8 (2021).

56. R. d. O. S. Wanderley, R. M. F. de Figueirêdo, A. J. d. M. Queiroz, et al., "The Temperature Influence on Drying Kinetics and Physico-Chemical Properties of Pomegranate Peels and Seeds," *Foods* 12, no. 2 (2023): 286.

57. V. R. Sagar and P. Suresh Kumar, "Recent Advances in Drying and Dehydration of Fruits and Vegetables: A Review," *Journal of Food Science and Technology* 47, no. 1 (2010): 15–26.

58. M. Kaveh, A. Jahanbakhshi, Y. Abbaspour-Gilandeh, E. Taghinezhad, and M. B. F. Moghimi, "The Effect of Ultrasound Pre-Treatment on Quality, Drying, and Thermodynamic Attributes of Almond Kernel under Convective Dryer Using ANNs and ANFIS Network," *Journal of Food Process Engineering* 41, no. 7 (2018).

59. S. A. Okaiyeto, S.-H. Yu, H. Wang, et al., "Vacuum-Steam Pulsed Blanching Enhances Drying, Nutrient Retention, and Anti-Nutritional Factor Reduction in *Vigna unguiculata*," *Food Chemistry* 495 (2025): 146343.

60. B. Sturm, A.-M. N. Vega, and W. C. Hofacker, "Influence of Process Control Strategies on Drying Kinetics, Colour and Shrinkage of Air Dried Apples," *Applied Thermal Engineering* 62, no. 2 (2014): 455–460.

61. F. Salehi and M. Kashaninejad, "Modeling of Moisture Loss Kinetics and Color Changes in the Surface of Lemon Slice During the Combined Infrared-Vacuum Drying," *Information Processing in Agriculture* 5, no. 4 (2018): 516–523.

62. P. B. Pathare, U. L. Opara, and F. A.-J. Al-Said, "Colour Measurement and Analysis in Fresh and Processed Foods: A Review," *Food and Bioprocess Technology* 6, no. 1 (2013): 36–60.

63. D. Zhang, D. Huang, Y. Zhang, et al., "Ultrasonic Assisted Far Infrared Drying Characteristics and Energy Consumption of Ginger Slices," *Ultrasonics Sonochemistry* 92 (2023): 106287.

64. A. A. Yamchi, R. Yeganeh, and A. Kouchakzadeh, "Effect of Ultrasonic Pretreatment on Drying Kinetics and Physio-Mechanical Characteristics of Peach Slices," *Journal of Food Process Engineering* 45, no. 8 (2022).

65. S. Kamiloglu, G. Toydemir, D. Boyacioglu, J. Beekwilder, R. D. Hall, and E. Capanoglu, "A Review on the Effect of Drying on Antioxidant Potential of Fruits and Vegetables," *Critical Reviews in Food Science and Nutrition* 56, no. sup1 (2015): S110–S129.

66. B. Nayak, R. H. Liu, and J. Tang, "Effect of Processing on Phenolic Antioxidants of Fruits, Vegetables, and Grains—a Review," *Critical Reviews in Food Science and Nutrition* 55, no. 7 (2015): 887–918.

Supporting Information

Additional supporting information can be found online in the Supporting Information section. **Supporting Information.** Supporting Figure 1(A). Experimental data and the best-fit predicted Midilli–Kucuk et al. model for all the drying condition at 40°C. Supporting Figure 1(B). Experimental data and the best-fit predicted Midilli et al. [30] model for all the drying condition at 50°C. Supporting Figure 1(B). Experimental data and the best-fit predicted Midilli et al. [30] model for all the drying condition at 60°C.